Surface Structure of CdSe Nanorods Revealed by Combined X-ray Absorption Fine Structure Measurements and ab Initio Calculations

Deborah M. Aruguete, Matthew A. Marcus, Liang-shi Li,† Andrew Williamson, Sirine Fakra, Francois Gygi,‡ Giulia A. Galli,§ and A. Paul Alivisatos*

Department of Chemistry, University of California at Berkeley, Berkeley, California 94720, Advanced Light Source, Lawrence Berkeley National Laboratory, Berkeley, California 94720, and Quantum Simulations Group, Lawrence Livermore National Laboratory, Livermore, California 94550

Received: September 13, 2006

We report orientation-specific, surface-sensitive structural characterization of colloidal CdSe nanorods with extended X-ray absorption fine structure spectroscopy and ab initio density functional theory calculations. Our measurements of crystallographically aligned CdSe nanorods show that they have reconstructed Cd-rich surfaces. They exhibit orientation-dependent changes in interatomic distances which are qualitatively reproduced by our calculations. These calculations reveal that the measured interatomic distance anisotropy originates from the nanorod surface.

Introduction

Surface structure and morphology play a key role in determining the physical and chemical properties of colloidal nanocrystals. For example, their rate of growth, size, and shape are influenced by the relative stability of different surface facets and the selective adhesion of surfactants.[1] In addition, in the case of semiconductor nanocrystals, the localization properties of surface electronic states and those of the potential confining the electrons are affected by the presence of organic capping groups.[2] Yet the characterization of the surfaces of colloidal nanoparticles remains a major experimental challenge. These surfaces are not atomically flat, posing great difficulties for the use of atomic scale scanning tunneling microscopy or low-energy electron diffraction techniques. The presence of multiple facets and edges further complicates measurements, and most current experimental techniques can only detect average properties.

In this work we use a combination of extended X-ray absorption fine structure (EXAFS) spectroscopy and density functional theory (DFT) calculations to investigate the surfaces of aligned colloidal nanorods. This combined approach allows one to observe surface relaxations along different crystallographic directions and to determine atomistic details of surface structure at the nanoscale.

Experimental Section

Preparation of Oriented Nanorod Assemblies for EXAFS. Liquid crystalline solutions of CdSe nanorods (3 nm diameter, 60 nm length) were prepared as described earlier,[3,4] in which the rods aligned parallel to each other along their *c*-axes. Throughout the experiment, the rods were kept air- and water-free. The nanorods are capped with alkylphosphonic acids and have the hexagonal wurtzite crystal structure; their long axes coincide with their crystallographic *c*-axes.[1] Control samples with unoriented rods were prepared in a similar manner.

EXAFS Spectroscopy and Data Analysis. Se K-edge XAS was collected from the CdSe rods at Advanced Light Source beamline 10.3.2 (Berkeley, CA), using a 16 μm (horizontal) × 7 μm (vertical) μm beam spot.[5] This small spot size allowed us to collect data from a single domain of oriented nanorods. We then rotated the sample to measure XAS at multiple rod orientations with respect to the polarization of the X-rays (Figure 1C; see Figure S1 (Supporting Information) for raw dichroism data). XRD was collected before and after each acquisition of XAS for each rod orientation, both to determine the orientation distribution and to ensure that no shift occurred during measurement (orientation distributions are contained in Table S1 of the Supporting Information). Nanorod samples were cooled to −50 °C in order to prevent such shifts. Bulk standards were measured at room temperature. Fourier transform magnitudes of the data from bulk standards and nanorods are shown in Figure S2 (Supporting Information).

The EXAFS data were subjected to background subtraction, normalization, conversion to *k*-space with k^2 weighting, and Fourier-filtering per a previously reported procedure.[6] To obtain structural parameters (e.g., interatomic distances *r*, coordination numbers (CNs), and mean squared distance displacements, or distribution of interatomic distances σ^2), the filtered nanorod spectra were fit to reference data. Bulk first nearest-neighbor distance (1NN) data were used as the 1NN reference. Second (2NN) and third (3NN) nearest-neighbor distance references were derived from bulk CdSe data, elemental Se data, and scattering calculations with FEFF 8.1.[7,8]

Due to the uniaxial symmetry of the nanorods, for small changes we can express the angular dependence of an interatomic distance *r* within a given atomic coordination shell as

$$\bar{r}(\theta) = (r_{||} - r_{\perp})\langle\cos^2\theta\rangle + r_{\perp}, \quad (1)$$

which is valid for a sample whose apparent coordination number is angle-independent, as in our case.[9] Here θ is the angle

* Corresponding author. E-mail: alivis@berkeley.edu. Phone: (510) 643-7371. Fax: (510) 642-6911.
† Current address: Indiana University, Department of Chemistry, Bloomington, IN 47405.
‡ Current address: Department of Applied Science, University of California at Davis, Davis, CA 95616.
§ Current address: Department of Chemistry, University of California at Davis, Davis, CA 95616.

10.1021/jp065986z CCC: $37.00
Published on Web 12/06/2006

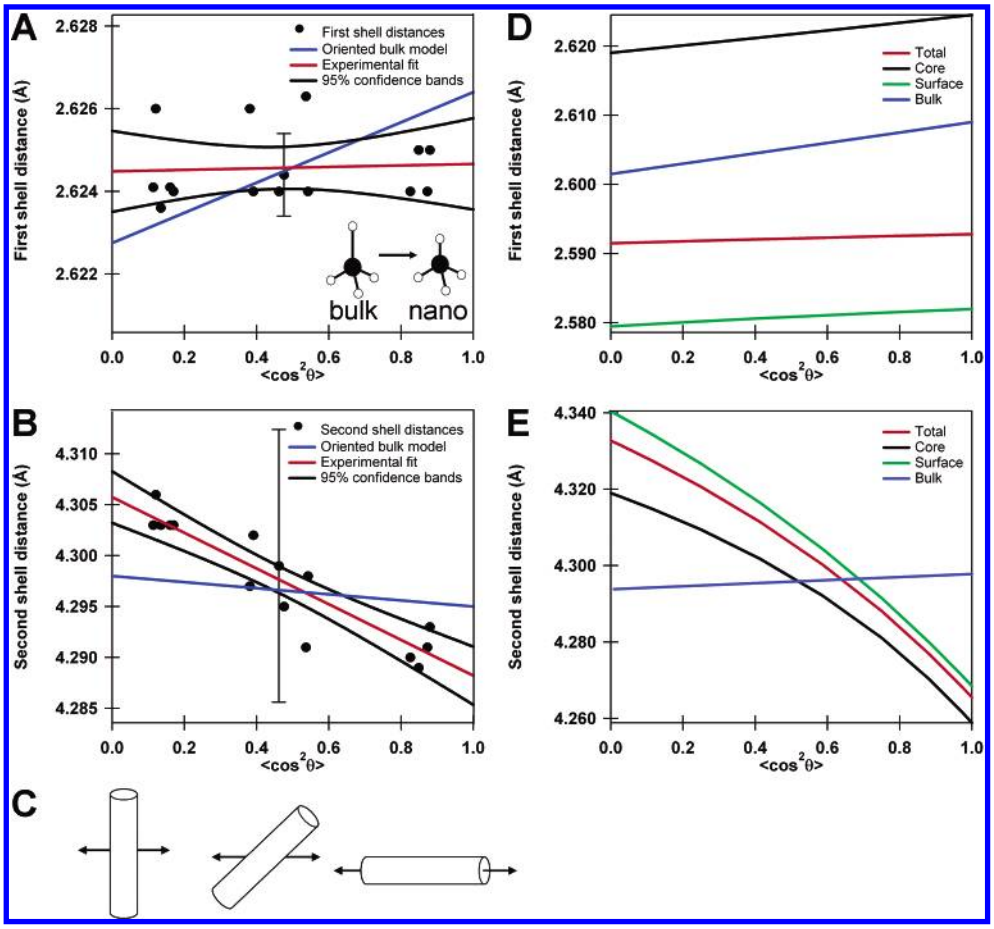

Figure 1. A. Cd−Se distances (first shell) versus $\langle \cos^2 \theta \rangle$. Inset: schematic drawing of $SeCd_4$ tetrahedron in nanorods and bulk showing loss of distortion in nanorods. B. Se−Se distances (second shell) versus $\langle \cos^2 \theta \rangle$. For both A and B, the black curves denote the 95% confidence bands, while the blue lines are calculated for an oriented ideal bulk crystal of CdSe. The experimental fits are shown in red. The error bars displayed in each of these plots are representative of the systematic error in each distance measurement. C. Schematic of nanorod orientation with respect to the X-ray polarization, denoted by the double-headed arrow. D. Plot of $\cos^2 \theta$-weighted Cd−Se distances from DFT calculation of a relaxed nanorod versus $\cos^2 \theta$. E. Plot of $\cos^2 \theta$-weighted Se−Se distances from DFT calculation of a relaxed nanorod versus $\cos^2 \theta$. The green lines denote the surface nanorod distances, the black lines are the core nanorod distances, and the red lines the average of all distances. The blue lines are bulk CdSe distances derived from the DFT calculation. In A and E the oriented bulk model data are shifted downward by 0.007 Å and upward by 0.04 Å, respectively, for a better visual comparison.

between the X-ray beam polarization and the nanorod *c*-axes, and the angle brackets denote an orientational average over the rods, derived experimentally with XRD. $\bar{r}(\theta)$, the measured value of r at a given value of θ, is a weighted sum of axial distances (along the *c*-axis) and equatorial distances (along the *a*-/*b*-axes); hence, axial and equatorial distances are not individually resolved. $r_{||}$ and $r_{\perp}$ are the extrapolated values of r when the rod *c*-axes are parallel and perpendicular to the beam polarization, respectively, and are weighted sums of axial and equatorial distances as well. We define the anisotropy in r as the difference $r_{||} - r_{\perp}$. Linear relationships with respect to $\langle \cos^2 \theta \rangle$ similar to eq 1 can also be applied to atomic coordination numbers and mean-squared relative distance displacements.

Using eq 1, we derived anisotropies for 1NN distances (Cd−Se bond lengths) and 2NN distances (Se−Se distances). Results from these fitting procedures were confirmed by an alternative corefinement fit, in which we fit data from all angular orientations simultaneously, thus maximizing the ratio of the degrees of freedom to the number of fitting parameters (see Tables S2 and S3 in the Supporting Information for the results of these fits). We also attempted to add asymmetry in interatomic distance distributions to the radial distribution functions derived for 1NN and 2NN shells, but this did not yield a consistent improvement of the fit. This may stem from the use of room-temperature reference data for bulk CdSe, which already contain anharmonicity effects with respect to zero T data. We also analyzed data from a control study on nonaligned rods, using the same procedures discussed above, to ensure that the dichroism measured for the oriented rods did not originate from spurious effects.

Ab Initio Calculations. To understand the structural origin of the EXAFS measurements, we performed a series of first principles, density functional theory (DFT) electronic structure calculations. A complete 3 nm × 60 nm CdSe nanorod contains approximately 16 000 atoms, which is too many for practical ab initio simulation from first principles. Instead, we model the nanorods as infinitely long nanowires which are periodic along the [0001] direction (long axis). Our structural model (Figure 2) is a 2.4 nm diameter nanowire, with (1000) and (1−100) side facets. The electronic structure of the nanowire and a reference bulk structure were calculated using the Qbox[10] and ABINIT[11] ab initio molecular dynamics and pseudopotential DFT codes, respectively. All calculations were performed using the local density approximation (LDA), with the Ceperley−Alder exchange-correlation functional.[12] The wavefunctions were expanded in a plane wave basis, with a 35 Ry energy cutoff with 4 *k*-points along the [0001] direction in the nanowire. Norm conserving, Troullier−Martins pseudopotentials, with $4d^{10}5s^2$

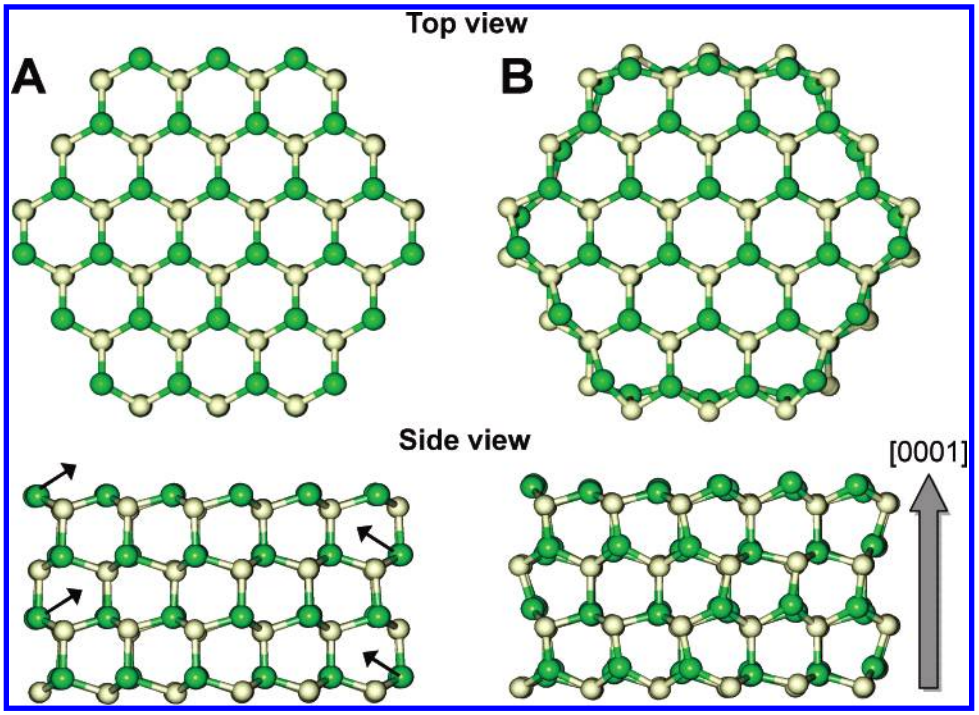

Figure 2. Top views and side views of the unrelaxed (A) and relaxed (B) 2.4 nm diameter CdSe nanowire structures obtained from DFT calculations. The side view shows two periodic repeat units of the structure. Green atoms are Cd, white atoms are Se. The core atomic positions are mostly unchanged, while the outer atoms shift. The relaxation of the surface Cd atoms is highlighted by arrows.

and $4s^2 4p^4$ valence electrons were used to represent the Cd and Se cores, respectively. For both the bulk and nanowire systems the atomic coordinates were relaxed to their closest, lowest energy atomic positions, with forces less than 5×10^{-4} eV/Å. The dimensions of the simulation supercells were also relaxed to their lowest energy configurations to allow for changes in the structural parameters *c*, *u*, and *a*, where *u* is the ratio of the nearest-neighbor distance along the *c*-axis to *c*.

Results and Discussion

Orientation-Dependent Variation of Interatomic Distances. EXAFS Measurements. Plots of *r* versus $\langle \cos^2 \theta \rangle$ are shown in Figure 1 for both the 1NN and 2NN distances, along with the results of least-squares linear fits, including 95% confidence bands. The orientation of the rods with respect to the beam polarization is depicted schematically as well. Also shown in these plots are the bulk CdSe model data. Bulk CdSe does not have perfectly isotropic, tetrahedral bonding; the axial 1NN and 2NN distances are elongated and reduced, respectively, by 0.005 Å. The error caused by neglecting these differences when using the bulk powder as a model is negligible (see Supporting Information). The nanorods do not show the 1NN distance distortion (Figure 1A, inset) as evident from the lack of anisotropy shown in Figure 1A; $(r_{||} - r_{\perp})_{nano} = 0.000(\pm 0.001)$ Å, while $(r_{||} - r_{\perp})_{bulk} = 0.004$ Å. However, the 1NN distances were nearly the same as the bulk ($r_{1NN,nano} = 2.625 \pm 0.001$ Å; $r_{1NN,bulk} = 2.630$ Å; bulk model data is shifted in Figure 1A for a better visual comparison with nanorod data). Nanorod axial 2NN distances are reduced to $4.282(\pm 0.005)$ Å ($r_{2NN,bulk,axial} = 4.293$ Å); equatorial (along *a*/*b*-axes) 2NN distances are closer to those in the bulk ($r_{2NN,nano,equatorial} = 4.304 \pm 0.004$ Å, $r_{2NN,bulk,equatorial} = 4.298$ Å). There is a significantly observable 2NN distance anisotropy of -0.018 ± 0.012 Å (Figure 1B). All bulk distances cited[13] were adjusted for the experimental temperature.[14] In these fits, it should be noted that the precision of distance determinations is considerably better than the absolute accuracy, because we are comparing samples that are structurally very similar to each other (namely, nanorod liquid crystals measured at different orientations). Thus, we can see small distance changes between measurements at different orientations, even if we cannot measure an absolute distance to better than $\sim \pm 0.015$ Å. We observed no orientational dependence in our measurements of atomic coordination numbers or mean-squared relative distance displacements.

Comparison of Measured and Calculated Interatomic Distances. The ideal and relaxed nanowire structures are shown in Figure 2. We find that the core of the nanowire undergoes relatively minor structural relaxations from the ideal bulk wurtzite structure, while the surface of the nanowire spontaneously reconstructs to lower its energy. In particular, surface atoms with a coordination number of 2 undergo the most dramatic structural relaxations, wherein Se−Cd U-shaped structures rotate so that the Cd atoms move into the surface of the wire, increasing their coordination. This rotation is highlighted with arrows in Figure 2. Similar surface relaxations have also been predicted for CdSe quantum dots.[15] After relaxation, the nanowire exhibits a broad distribution of bond lengths. The Cd−Se bonds in the core of the nanowire deviate from their bulk values by <1%, while those on the surface are altered by up to 5%.

To compare the DFT-predicted relaxed structures with the structures measured by EXAFS, in Figure 1D and 1E we plot the 1NN and 2NN anisotropy of the DFT relaxed structures. The qualitative changes in the anisotropy of both the 1NN and 2NN bonds are similar to those measured by EXAFS. For the 1NN, the relaxed bulk structure (blue line) exhibits a positive anisotropy (elongation) along the *c*-axis, while the relaxed nanowire (red line) exhibits almost no anisotropy, as was observed with EXAFS. For the 2NN the bulk structure exhibits a small elongation along the *c*-axis, while the nanowire exhibits a strong negative anisotropy, with smaller 2NN bond lengths along the *c*-axis, again in agreement with EXAFS measurements.

In addition to predicting the total change in anisotropy when moving from a bulk to nanowire geometry, the atomistic simulations can investigate the structural origin of the anisotropy. In Figures 1D and 1E, we separate the contributions to 1NN and 2NN anisotropy from atoms in the core (black lines) and on the surface (green lines) of the nanowires. This analysis shows that the core 1NN bonds expand by ~1% compared to the bulk and show a small positive anisotropy, while the surface bonds contract by ~0.5% and do not show any anisotropy. In contrast, both the core and surface 2NN Se−Se bonds show a strong negative anisotropy, arising from an expansion of 2NN distances perpendicular to the *c*-axis.

We note that while the calculated and measured trends in bond lengths show good agreement, the DFT predicted bond lengths are approximately 1% shorter than the measured ones. This underestimate of the CdSe bulk bond length has been observed in previous calculations[16,17] and results from known "overbinding" in semiconductors and insulators when described within the local density approximation of DFT. We also note that the measured and predicted structural anisotropies qualitatively agree, even though no surfactant molecules were included in the DFT simulations. This result supports previous theoretical predictions,[15] indicating that the interaction between surfaces of small CdSe dots and organic surfactants is weak enough not to significantly perturb surface relaxations obtained for bare dots. Previous calculations on bulk CdSe surfaces indicated that surfactants will reduce surface relaxations,[18] which may explain why the DFT calculations presented here predict a larger 2NN anisotropy than measured.

The observed compression of CdSe nanorods along their *c*-axes appears to depend not only on their size, but their shape. II−VI quantum dots of comparable size have displayed decreased bond distances with respect to the bulk.[19] A study on CdSe nanodots showed that both the *c*- and *a*-axes were compressed,[20] rather than just the *c*-axis. Bulk CdSe mechanical properties do not explain the anisotropic compression in the nanorods, as the elastic modulus along the *c*-axis (87.1 GPa) is larger than that along the *a*-axis (74.6 GPa).[21] As neither size nor bulk properties explain the preferential *c*-axis compression, we conclude that the origin of this compression must lie in the rod shape. This is consistent with structural studies on other anisotropic nanomaterials, such as colloidal core−shell CdSe−ZnS nanorods. As the ZnS shell thickness was increased, XRD revealed an overall compression which was maximal along the *c*-axis.[22] Wurtzite GaN and ZnO nanowires[23,24] also displayed asymmetric changes in atomic distances, although their anisotropy was of the opposite sign of the one observed here (their long axes stretched, while their short axes shrank). Bulk ZnO deviates more from perfect tetrahedral bonding than nanowire ZnO,[24] similar to what occurs in CdSe. However, when comparing the behavior of ZnO and GaN with that of CdSe rods, it is important to note that both of these nanowire materials were grown differently than the CdSe nanorods, in particular, with no surfactants.

Se Atomic Coordination on Nanorod Surfaces. Finally, we have also investigated the CN of the Se atoms in the nanorods as a probe of the Cd content on the nanorod surfaces. Our measured 1NN and 2NN CNs are 3.6 (±0.05) and 9.98 (+0.96, −0.72), respectively. These CNs fall in between those expected for a completely Cd-terminated wire (4, 9.94) and those expected for a stoichiometric wire (3.4, 10.1), indicating, as expected, a slightly Cd-rich surface. These results are consistent with Rutherford backscattering spectroscopy performed on CdSe dots synthesized in a similar manner.[25] Additionally, we observe no angular dependence of the 1NN and 2NN CNs in the nanorods. This is consistent with nanorod models based on the ideal wurtzite lattice structure, which predict that the angular dependence averages to zero when the contributions from all surface facets of a cylindrical rod are included.

As the surface is not entirely Cd-coated, we explored the possibility of having other atoms bound to Se. Data fits did not improve when including the shells from reference compounds of likely surface species, indicating that the only atom bound to Se is Cd. Thus, there is probably unpassivated Se on the nanorod surfaces, which agrees with previous theoretical and experimental work on quantum dots.[18,26]

Conclusions

In conclusion, we have used a combination of EXAFS measurements and DFT calculations to characterize the structure and surfaces of CdSe nanorods. We found that, in the rods, 1NN and 2NN distances are reduced along the *c*-axis with respect to bulk CdSe, while distances along the *a*/*b*-axes are mostly unchanged. DFT predictions for the relaxed structures qualitatively agree with these measurements. In addition, our calculations indicate that the most significant structural changes accounting for the measured anisotropy occur on the surface of the nanowires. Further comparisons between nanowire models and our measurements show that the nanorod surfaces are Cd-rich, with some unpassivated Se atoms. This investigation shows that EXAFS measurements, combined with ab initio calculations, represent a powerful tool to investigate surface relaxations at the nanoscale.

Acknowledgment. We thank Dr. Can Erdönmez, Dr. Benjamin Boussert, and Dr. Benjamin Gilbert for useful discussions. This work was supported by the DOD Advanced Research Projects Agency (DARPA) through the Univ. of Southern California subaward agreement 066995. Additional support came from the Director, Office of Science, Office of Basic Energy Sciences, of the U.S. DOE under Contract No. DE-AC03-76SF00098, and NSF grant DMR-0238760. The LLNL work was performed under the auspices of the US Department of Energy by the University of California, Lawrence Livermore National Laboratory under contract No. W-7405-Eng-48.

Supporting Information Available: Fourier transform magnitudes of data from bulk standards and nanorods, raw anisotropy data, nanorod orientational distributions (derived from X-ray diffraction), and additional details about EXAFS fitting. Fourier transform magnitudes derived from FEFF 8.1 calculations on nanowire simulations are also included. This material is available free of charge via the Internet at http://pubs.acs.org.

References and Notes

(1) Manna, L.; Scher, E. C.; Alivisatos, A. P. *J. Am. Chem. Soc.* **2000**, *122*, 12700.

(2) Talapin, D. V.; Rogach, A. L.; Kornowski, A.; Haase, M.; Weller, H. *Nano Lett.* **2001**, *1*, 207.

(3) Li, L. S.; Walda, J.; Manna, L.; Alivisatos, A. P. *Nano Lett.* **2002**, *2*, 557.

(4) Li, L. S.; Alivisatos, A. P. *Adv. Mater.* **2003**, *15*, 408.

(5) Marcus, M. A.; MacDowell, A. A.; Celestre, R.; Manceau, A.; Miller, T.; Padmore, H. A.; Sublett, R. E. *J. Synchrotron Radiat.* **2004**, *11*, 239.

(6) Marcus, M. A.; Manceau, A.; Kersten, M. *Geochim. Cosmochim. Acta* **2004**, *68*, 3125.

(7) Rehr, J. J.; Albers, R. C. *Rev. Modern Phys.* **2000**, 621.

(8) Ankudinov, A. L.; Ravel, B.; Rehr, J. J.; Conradson, S. D. *Phys. Rev. B: Condens. Matter* **1998**, *58*, 7565.

(9) Koningsberger, D. C.; Prins, R. *X-Ray Absorption: Principles, Applications, Techniques of EXAFS, SEXAFS, and XANES*; John Wiley and Sons: New York, 1988; Vol. 92.

(10) Gygi, F. *The Qbox code*; Lawrence Livermore National Laboratory: Livermore, CA.

(11) The ABINIT code is a common project of the Universite Catholique de Louvain, Corning Incorporated, and other contributors (http://www.abinit.org).

(12) Ceperley, D. M.; Alder, B. J. *Phys. Rev. Lett.* **1980**, *45*, 566.

(13) Stevenson, A. W.; Barnea, Z. *Acta Crystallogr. B* **1984**, *40*, 530.

(14) *Thermal expansion−nonmetallic solids*; Touloukian, Y. S.; Kirby, R. K.; Taylor, R. E.; Lee, T. Y. R., Eds.; Plenum: New York, 1977; Vol. 13.

(15) Puzder, A.; Williamson, A. J.; Gygi, F.; Galli, G. *Phys. Rev. Lett.* **2004**, *92*, 217401.

(16) Yeh, C.; Lu, Z. W.; Froyen, S.; Zunger, A. *Phys. Rev. B: Condens. Matter* **1992**, *46*, 10086.

(17) The underestimate of the bulk CdSe lattice constant predicted by the LDA to DFT is a small, systematic error (a known drawback of the LDA). In both the bulk and nanorod structures we took this into account by a rescaling of the calculated EXAFS spectra, when comparing to the measured, bulk spectra. This rescaling does not affect in any way the extraction of information on the surface relaxation of the nanowires, as obtained from DFT calculations; indeed this information is contained in the relative magnitude of the peaks in the EXAFS spectra, and it is unaffected by the rescaling that we have applied.

(18) Manna, L.; Wang, L. W.; Cingolani, R.; Alivisatos, A. P. *Journal of Physical Chemistry B* **2005**, *109*, 6183.

(19) Rockenberger, J.; Troeger, L.; Kornowski, A.; Vossmeyer, T.; Eychmueller, A.; Feldhaus, J.; Weller, H. *Journal of Physical Chemistry B* **1997**, *101*, 2691.

(20) Zhang, J.-Y.; Wang, X.-Y.; Xiao, M.; Qu, L.; Peng, X. A*pplied Physics Letters* **2002**, *81*, 2076.

(21) *Landolt-Bornstein−Condensed Matter: II-VI and I-VII Compounds; Semimagnetic Compounds*; Rossler, U., Ed.; Springer-Verlag GmbH, 1999; Vol. 41, pp 721.

(22) Manna, L.; Scher, E. C.; Li, L. S.; Alivisatos, A. P. *J. Am. Chem. Soc.* **2002**, *124*, 7136.

(23) Seo, H. W.; Bae, S. Y.; Park, J.; Yang, H.; Park, K. S.; Kim, S. *J. Chem. Phys.* **2002**, *116*, 9492.

(24) Han, S. W.; Yoo, H. J.; An, S. J.; Yoo, J.; Yi, G. C. *Appl. Phys. Lett.* **2005**, *86*.

(25) Taylor, J.; Kippeny, T.; Rosenthal, S. J. *J. Cluster Sci.* **2001**, *12*, 571.

(26) Katari, J. E. B.; Colvin, V. L.; Alivisatos, A. P. *J. Phys. Chem.* **1994**, *98*, 4109.